Available online at www.sciencedirect.com
SCIENCE DIRECT®

Continental Shelf Research 25 (2005) 1–6

CONTINENTAL SHELF RESEARCH

www.elsevier.com/locate/csr

Infrared imagery of large-aspect-ratio Langmuir circulation

G.O. Marmorino*, G.B. Smith, G.J. Lindemann

Code 7230, Remote Sensing Division, Naval Research Laboratory, Washington, DC 20375-5320, USA

Received 3 June 2004; received in revised form 16 August 2004; accepted 27 August 2004
Available online 5 November 2004

Abstract

Airborne infrared imagery collected off the West Florida coast reveals Langmuir circulation patterns having across-wind spacings of the order of ten times the local water depth. This implies a much flatter circulation cell than has been typically reported but supports observations made off the Texas coast by Hunter and Hill (Remote Sensing Environ. 10 (1980) 115). The conditions under which such large-aspect-ratio circulation cells form remain unclear.
Published by Elsevier Ltd.

Keywords: Langmuir circulation; Infrared imagery; West Florida Shelf

1. Introduction

Langmuir circulation (Lc) is commonly observed on the surface of the ocean as a quasi-regular pattern of streaks or windrows, roughly aligned with the wind. These are the surface signatures of an array of subsurface counter-rotating vortices, or cells, and are often made visible by the accumulation of buoyant material and natural films in the regions of surface convergence. Individual streaks are often observed to either terminate or merge with their neighbors, and there appears to be a preference for merging streaks to form a 'Y' shape with the open end upwind (Farmer and Li, 1995). The unsteadiness and complexity of the resulting network of streaks contribute substantially to the across-wind dispersion of floating material such as oil (e.g., Thorpe, 2004). Lc is also a major factor in vertical mixing and this effect needs to be appropriately incorporated into models of atmosphere–ocean exchange. Therefore, understanding the spatial scales of Lc is of great practical importance.

There is generally a hierarchy of horizontal scales associated with Lc, but most existing field measurements show the largest streak spacing, s, to be of the order of three times the depth, h, of the surface mixed layer. A value of $s/h \approx 3$ implies an aspect ratio of 1.5 for an individual cell. A similar aspect has been found where Lc extends to the bottom (e.g., van Straaten, 1950; Gargett and Wells, 2004), in which case h is taken to be the

*Corresponding author.
E-mail address: marmorino@nrl.navy.mil
(G.O. Marmorino).

0278-4343/$ - see front matter Published by Elsevier Ltd.
doi:10.1016/j.csr.2004.08.002

bottom depth. An exception to this usual result seems to have been observed by Hunter and Hill (1980). These authors observed bands of turbid water in aerial color photographs of the inner Texas shelf (water depths of 6–14 m) and deduced that the bands must be produced by the rising of suspended particles from the bottom along lines of *bottom* convergence. As they point out, the observed orientation of the bands with respect to the wind and occurrence of downstream *separation* of bands appear to be consistent with Lc, except that the bands had a mean spacing of ten times the water depth. This implies circulation cells having an aspect ratio of five, which would be the largest value ever reported in field measurements.

The purpose of the present note is to report observations of surface temperature patterns, made over the inner West Florida Shelf, that support Hunter and Hill's tentative conclusion that large-aspect-ratio Lc can indeed occur, though under circumstances that are still unclear. Our data were collected using an airborne mid-band (3–5 μm wavelength) infrared camera on 15 December 2002 (Table 1). At these wavelengths only radiation either emitted by or scattered from the water surface reaches the camera, enabling the extraction of thermal information from the imagery. The windrows appear in the imagery due to the effects of the underlying hydrodynamics on a thin surface thermal boundary layer, or 'cool skin'. In the regions of surface convergence this layer thickens and the accumulation of surface film damps turbulence in the underlying water. Both these effects lower the surface temperature so that convergence regions appear dark in the infrared (McLeish, 1968; see also Marmorino et al., 2004). Passes were made at altitudes of 1500 and 165 m, providing surface resolutions of 3.4 and 0.4 m. While no in situ measurements are available from within the study area, some estimate of current, water stratification, and wave conditions can be made from the imagery; and measurements of the wind and sensible heat flux are available from a site 15 km away (Table 1).

2. Results

Fig. 1 shows imagery from a high-altitude pass made near the mouth of Tampa Bay, extending from the area east of Egmont Key, northward over the 30-m-deep Egmont Channel, and continuing onto a shallow inner shelf region where the Lc patterns occur. These patterns consist of dark streaks that correspond to lower surface temperatures. Compared to the water between them, the streaks in this figure appear cooler by about 0.03 °C, which is just above the resolution of the infrared camera. The streaks have a mean spacing of about 20 m, or about 10 times the mean water depth of approximately 2.1 m. (The water depth ranges from about 1.2 m at the lip of the Egmont channel to 3 m at the northern edge of the image.) The streaks have a mean orientation of 345°T and so approximately align with the wind, which was from 352°T at 5.5 m/s (Table 1). Another striking

Table 1
Time, aircraft altitude and heading, wind direction and speed, surface heat flux, and tidal stage corresponding to each of the figures

Fig.	Time (UT)	Altitude (m)	Heading (°T)	Wind direction (°T)	Wind speed (m/s)	Heat flux (W/m^2)	Tidal stage (h)
1	2347	1528	4	352	5.5	−235	3.6
2a	2335	168	347	342	5.9	−235	3.4
2b	2325	170	345	342	5.9	−235	3.2
3	2200	155	348	340	4.2	−210	−3.2

Winds at 10-m height were measured 15 km east–northeast of the study area at a tower operated by the University of South Florida (see http://comps.marine.usf.edu/BRACE/). Local sunset occurred at 2242 UT. The surface heat flux (negative values indicate heat loss from the water; uncertainty of the order of 20%) was calculated using measurements at the tower of sensible heat flux, vapor pressure, and air temperature. The air–sea temperature difference was about −5 °C. Estimates of the water temperature at the site and at the tower show only a 0.3 °C difference; therefore the tower-based heat flux should be a good estimate of the flux at the study site. Tidal stage is in hours relative to high tide (maximum flood) at Egmont Key. The tidal range over Egmont Channel is less than 0.3 m.

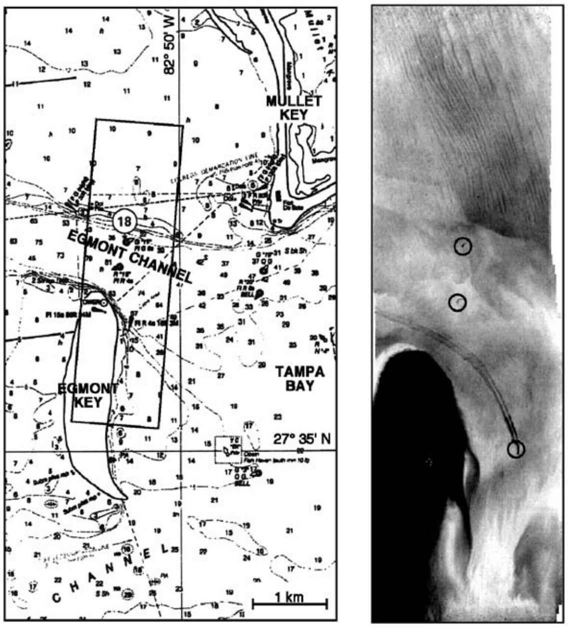

Fig. 1. Study location (soundings in feet) with rectangle showing area of infrared imagery (right). Langmuir circulation patterns appearing north of Egmont Channel are the focus of the paper. Darker shades in the imagery indicate lower surface temperatures. Image width is 1130 m. Three black circles drawn on the imagery highlight two channel buoys and a small boat that was steaming around the northern part of Egmont Key, leaving two dark bands (likely foam bands) along its wake.

feature in the imagery is the coherence of the streaks. Individual streaks extend over about 1 km, or about 50 times the spacing. A second high-altitude pass (not shown) made farther to the east shows the pattern of streaks extending to within 200 m of Mullet Key. The southern boundary of the Lc pattern lies along the edge of Egmont Channel, where there is also a temperature front (see below). An additional area of widely spaced streaks can be seen east of Egmont Key in water depths of 2–4 m. The remainder of the paper focuses on the area north of Egmont Channel as that area was also sampled at lower altitude, affording a higher-resolution view of the patterns.

Fig. 2 shows imagery from two successive low-altitude passes. The streaks are now well resolved and can be seen to have a width of about 2 m, or roughly 10% of the mean spacing. Also, the contrast of the streaks is now larger, about 0.14 °C cooler than ambient. The actual temperature of the streaks has not changed; rather, at the lower altitude the image resolution is improved and the atmospheric attenuation is greatly reduced, both effects acting to increase the signal. A close examination of the figure also reveals additional streaks lying between and at a small angle to the major ones. These have a spacing of only a few meters and may represent a second scale of Lc (cf. Thorpe, 1992). In addition to streaks, bright (warm) patches occur throughout Fig. 2 and represent straining of the cool skin by

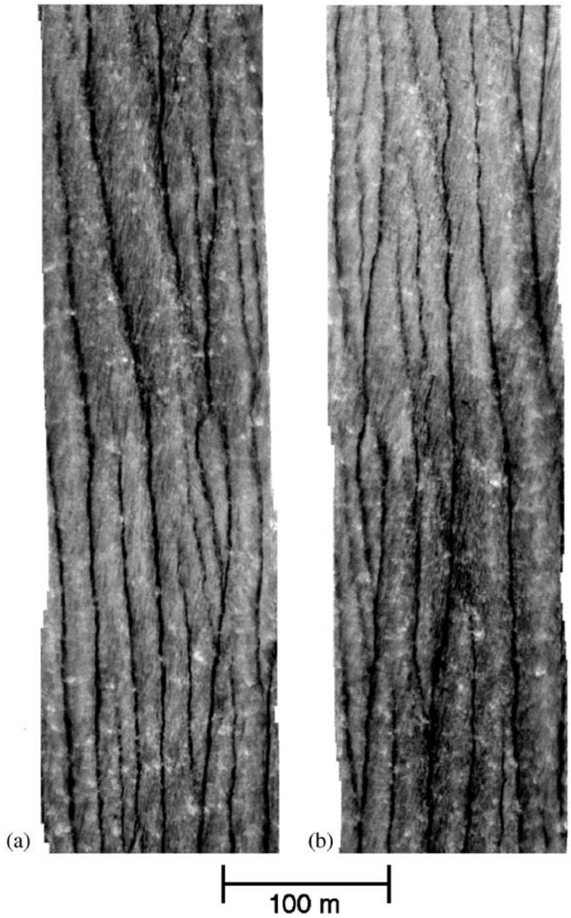

Fig. 2. Low-altitude imagery from the area north of Egmont Channel collected shortly before that in the previous figure. Strip (a) was acquired 10 min after strip (b). The imaged areas overlap by about 50%: the right half of (a) overlaps the left half of (b). The strips are shifted in the along-wind direction to align similar patterns. The temperature range is about 0.14 °C.

microbreaking, wind-generated surface waves (e.g., Jessup et al., 1997). Examination of 30-Hz image sequences shows the microbreaker crests oriented approximately normal to the streaks, which is consistent with the streaks being aligned with the local wind. Lines of microbreakers appear intermittently, and their separation provides an estimate for the wavelength of the dominant surface waves of $\lambda \sim O(5\,\mathrm{m})$. A similar value was estimated from wave slope-induced reflections of sky radiation recorded during turns of the aircraft.

Fig. 2 shows multiple mergings of the widely spaced streaks into Y-shaped junctions. These Y-junctions open toward the top of the image, which is the upwind direction. The typical angle included by a Y-junction in our data is about 15°, about half that measured by Farmer and Li (1995) in the Georgia Strait, though under much higher winds ($>12\,\mathrm{m/s}$). There are also examples in Fig. 2 of individual streaks terminating at their downwind ends and new streaks apparently arising spontaneously upwind. As the two passes shown in the figure partially overlap and were made only 10 min apart, nearly identical spatial patterns appear in both Fig. 2a and b. These patterns drift downwind over time at an estimated 10 cm/s, and the strips in Fig. 2 have been shifted in the along-flight direction to more clearly indicate agreement in the structure of the patterns. Downwind translation of individual Y-junctions was also reported by Farmer and Li (1995).

Fig. 3 is a low-altitude view of the southern boundary of the widely spaced streaks, which occurs near the edge of Egmont Channel. The boundary clearly coincides with a weak temperature front ($\Delta T \approx 0.1\,^{\circ}\mathrm{C}$). Streaks in the warmer water south of the front have a spacing of only 2.5 m, but their orientation is similar to the wide streaks. The change in streak spacing occurs over a distance of only a few meters, suggesting a response to a change in stratification rather than

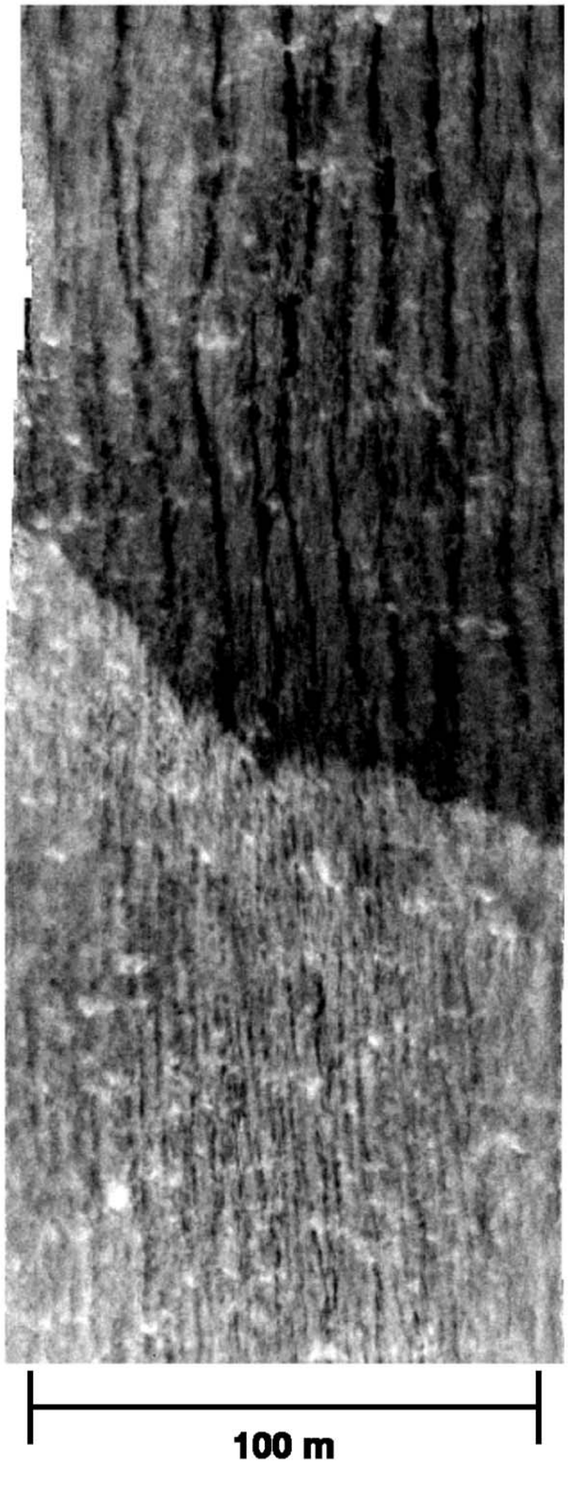

Fig. 3. Imagery showing change from wide to narrow spacing across a weak temperature front located along the northern edge of Egmont Channel. These data were collected 1.5 h before the examples in the previous figure. The temperature change across the front is about 0.1 °C.

to bathymetry. This suggests that the narrowly spaced streaks are depth-limited by stratification, implying stratified water south of the front and vertically well-mixed water to the north.

Additional observations of Lc in the area north of Egmont Channel were made the previous evening (0100 UT, 15 December). Though the wind was stronger (about 8 m/s) and breaking waves more energetic, the spacing of the streaks was in the range of 16–20 m and so comparable to the imagery shown.

3. Discussion

The infrared patterns we observed exhibit many of the usual characteristics associated with Lc: e.g., streaks aligned with the wind, Y-shapes opened upwind, and persistence of patterns. The only unusual feature is the large spacing-to-depth ratio of the order of 10. As this value is comparable to that found by Hunter and Hill (1980), our results support their tentative interpretation of such patterns as being consistent with Lc. We can further note that Hunter and Hill observed streak coherence lengths of 1 km or more, which is similar to our observations.

Possible issues contributing to the formation of relatively wide Lc cells were considered by Hunter and Hill (1980). They suggest that penetration of the circulation to the bottom boundary and a lateral boundary that limits the horizontal flow might be important factors. However, van Straaten (1950) observed bottom-penetrating Lc occurring in narrow tidal channels up to several meters in depth and found a typical value of s/h of only 3, suggesting that these two factors are insufficient. Hunter and Hill also note Faller and Caponi's (1978) result that in shallow water values of s/h can exceed 3, provided the surface gravity waves have a wavelength λ that is of the order of five times the water depth h. However, in our case we estimate λ as being only about twice h.

Could the structures we observed be the signatures of unstable convection cells in the water, converted into two-dimensional form by vertical shear as in the case of two-dimensional rolls in the atmosphere? Such rolls typically have an aspect ratio of around 3–4 but have occasionally been observed to have an aspect ratio as large as 20, though why such large values should occur is not well understood (see the review by Atkinson and Zhang, 1996). For the ocean case, the relative importance of convective or buoyancy forcing compared with wave forcing (through Stokes drift) can be estimated from the Hoenikker number, which can be written approximately as (Li and Garrett, 1995)

$$Ho \approx -(7 \times 10^{-4})Q/U_{\mathrm{w}},$$

where Q is the surface heat flux and U_{w} is the 10-m-height wind speed. At the time the data shown in Fig. 1 were collected, $Q \approx -235\,\mathrm{W/m^2}$ and $U_{\mathrm{w}} \approx 5.5\,\mathrm{m/s}$ (Table 1), so Ho is estimated to be about 0.03. This small value suggests that convection due to the surface heat loss is relatively unimportant in driving the Lc (Li and Garrett, 1995; Thorpe, 2004) and should therefore have little effect on the strength and form of the resulting circulation. An explanation in terms of thermally unstable shear flow therefore seems unlikely.

Numerical simulations of Lc suggest that, under appropriate forcing conditions, cells non-linearly cascade to some large but finite size. Cox and Leibovich (1993) considered a mixed layer having an impenetrable, constant-stress bottom boundary. While their model ignores many effects that may be important, we can use this as a first approximation to a solid bottom boundary. They found that as long as the surface waves produce a Stokes drift having a depth scale δ that is not small compared to the layer depth, the preferred spacing of the streaks will be large compared to the layer depth. For example, their Fig. 5 shows a result having $s/h = 2\pi$. The depth scale can be estimated as $\delta = 0.12U_{\mathrm{w}}^2/g$, where g is the gravitational acceleration and the wave spectrum is assumed to be fully developed (Li and Garrett, 1993). For our data, $\delta \approx 0.4\,\mathrm{m}$, making $\delta/h \approx 0.2$; for Hunter and Hill's (1980) data, we estimate δ/h as being of the order of 0.1. While these values appear compatible with the theory, it is still unclear how to reconcile the relatively widely spaced signatures we and Hunter and Hill (1980) have observed with measurements showing much smaller values of aspect ratio. It is important to resolve this issue so that the surface expressions of Lc can be properly interpreted and the conditions under which Lc penetrates to the bottom understood. With a more complete understanding, high-resolution imagery (such as the infrared imagery we have presented) can be used to investigate a range of broad questions relating to turbulence in shallow water, sediment resuspension and transport, and benthic ecology.

Acknowledgments

This work was supported by the Office of Naval Research through PE-61153N (NRL WU 72-8179). We thank G. Chini for insightful discussion during the initial stage of this work.

References

Atkinson, B.W., Zhang, J.Wu, 1996. Mesoscale shallow convection in the atmosphere. Reviews of Geophysics 34, 403–431.

Cox, S.M., Leibovich, S., 1993. Langmuir circulation in a surface layer bounded by a strong thermocline. Journal of Physical Oceanography 23, 1330–1345.

Faller, A.J., Caponi, E.A., 1978. Laboratory studies of wind-driven Langmuir circulations. Journal of Geophysical Research 83, 3617–3633.

Farmer, D., Li, M., 1995. Patterns of bubble clouds organized by Langmuir circulation. Journal of Physical Oceanography 25, 1426–1440.

Gargett, A.E., Wells, J., 2004. Langmuir supercells, a dominant mechanism for sediment resuspension and transport in shallow shelf seas. Science, submitted for publication.

Hunter, R.E., Hill, G.W., 1980. Nearshore current pattern off South Texas—an interpretation from aerial photographs. Remote Sensing of Environment 10, 115–134.

Jessup, A.T., Zappa, C.J., Yeh, H., 1997. Defining and quantifying microscale wave breaking with infrared imagery. Journal of Geophysical Research 102, 23,145–23,153.

Li, M., Garrett, C., 1993. Cell merging and the jet/downwelling ratio in Langmuir circulation. Journal of Marine Research 51, 737–769.

Li, M., Garrett, C., 1995. Is Langmuir circulation driven by surface waves or surface cooling? Journal of Physical Oceanography 25, 64–76.

Marmorino, G.O., Smith, G.B., Lindemann, G.J., 2004. Infrared imagery of ocean internal waves. Geophysical Research Letters 21, L11309.

McLeish, W., 1968. On mechanisms of wind-slick generation. Deep Sea Research 15, 461–469.

Thorpe, S.A., 1992. The breakup of Langmuir circulation and the instability of an array of vortices. Journal of Physical Oceanography 22, 350–360.

Thorpe, S.A., 2004. Langmuir circulation. Annual Review of Fluid Mechanics 36, 55–79.

van Straaten, L.M.J.U., 1950. Periodic patterns of rippled and smooth areas on water surfaces, induced by wind action. Koninklijke Nederlandse Akademie van Wetenschappen Proceedings 53, 1217–1227.